



# Selenium Nanoparticles Synthesized Using *Pseudomonas stutzeri* (MH191156) Show Antiproliferative and Anti-angiogenic Activity Against Cervical Cancer Cells

This article was published in the following Dove Press journal:  
*International Journal of Nanomedicine*

Karthik Rajkumar <sup>1</sup>  
Sandhya MVS<sup>1</sup>  
Siva Koganti<sup>2</sup>  
Sandeepa Burgula <sup>1</sup>

<sup>1</sup>Department of Microbiology, Osmania University, Tarnaka, Hyderabad 500007, India; <sup>2</sup>Center for Advanced Research, Sri Venkateswara Institute of Medical Sciences, Tirupati 517507, India

**Purpose:** Selenium nanoparticles (SeNP) have several applications in the field of biotechnology, including their use as anti-cancer drugs. The purpose of the present study is to analyze the efficacy of green synthesis on the preparation of SeNP and its effect on their anti-cancer properties.

**Methods:** A bacterial strain isolated from a freshwater source was shown to efficiently synthesize SeNP with potential therapeutic properties. The quality and stability of the NP were studied by scanning electron microscopy, X-ray diffraction, zeta-potential and FTIR analysis. A cost-effective medium formulation from biowaste having 6% banana peel extract enriched with 0.25 mM tryptophan was used to synthesize the NP. The NP after optimization was used to analyze their anti-tumor and anti-angiogenic activity. For this purpose, first, the cytotoxicity of the NP against cancer cells was analyzed by MTT assay and then chorioallantoic membrane assay was performed to assess anti-angiogenic activity. Further, cell migration assay and clonogenic inhibition assay were performed to test the anti-tumor properties of SeNP. To assess the cytotoxicity of SeNP on healthy RBC, hemolysis assay was performed.

**Results:** The strain identified as *Pseudomonas stutzeri* (MH191156) produced phenazine carboxylic acid, which aids the conversion of Se oxyanions to reduced NP state, resulting in particles in the size range of 75 nm to 200 nm with improved stability and quality of SeNP, as observed by zeta ( $\zeta$ ) potential of the particles which was found to be  $-46.2$  mV. Cytotoxicity of the SeNP was observed even at low concentrations such as  $5 \mu\text{g/mL}$  against cervical cancer cell line, ie, HeLa cells. Further, neovascularization was inhibited by upto 30 % in CAMs of eggs coinoculated with SeNP when compared with untreated controls, indicating significant anti-angiogenic activity of SeNP. The NP also inhibited the invasiveness of HeLa cells as observed by decreased cell migration and clonogenic proliferation. These observations indicate significant anti-tumor and anti-angiogenic activity of the SeNP in cervical cancer cells.

**Conclusion:** *P. stutzeri* (MH191156) is an efficient source of Se NP production with potential anti-angiogenic and anti-tumor properties, particularly against cervical cancer cells.

**Keywords:** selenium nanoparticles, *Pseudomonas stutzeri*, MH191156, anti-angiogenic activity, clonal proliferation, cell migration, cervical cancer cells

Correspondence: Sandeepa Burgula  
Department of Microbiology, Osmania University, Tarnaka, Hyderabad 500007, India  
Tel +91-40-27090661; +9848056930  
Email s\_burgula@osmania.ac.in

## Introduction

Selenium is best known for its antioxidant activities. Selenium is a trace element required for the proper functioning of some enzymes in human body, such as glutathione peroxidase, thioredoxin reductase, and formate dehydrogenase.<sup>1</sup> High

doses of selenium in our body are toxic, and when ingested lead to many complications, such as diarrhoea, fatigue, hair loss, joint pain, and nausea. Microorganisms are capable of reducing these naturally occurring forms of selenium (selenite and selenite oxyanions) into their elemental forms. Microorganisms can be hardwired to produce nanoparticles of different shape, size, stability and conductivity by altering the desired parameters. These elemental forms of selenium nanoparticles are less toxic compared to their natural counterparts.<sup>2</sup> When taken in recommended doses, these nanoparticles help fight against certain types of cancers.<sup>3</sup> Although several studies have focused on selenium nanoparticles as an effective antioxidant,<sup>4,5</sup> recent studies have focused on the use of these nanoparticles tagged with other molecules for targeted drug delivery mechanisms to treat many cancers, serving as a means to<sup>6</sup> antagonize multidrug resistance among cancers.

Selenium nanoparticles are reported to kill cancer cells owing to their prooxidant behaviour inside these cells.<sup>7</sup> These nanoparticles are shown to induce ROS inside the cells, ultimately triggering the cells to undergo apoptosis. Previous studies have reported that SeNP inhibited the growth of cancer cells by arresting the cells in the S phase.<sup>8</sup> Addition of SeNP drastically decreased the lipid peroxidation, TNF-alpha levels, and C reactive protein levels in lung carcinoma.<sup>9</sup> Studies showed that SeNP also targets matrix metalloprotein 2 expression, thereby inhibiting metastasis in cancer cells.

Since the discovery of nanoparticles, several studies have been conducted to produce these efficient nanoparticles using a cost effective media.<sup>10</sup> Among these, considerable research has been performed in the past decade to produce nanoparticles using different parts of the plant. Nanoparticles have been shown to be synthesized especially using extracts from<sup>11</sup> leaves,<sup>12</sup> flower,<sup>13</sup> fruits,<sup>14</sup> seed and<sup>15</sup> stem.<sup>16</sup> This method of green synthesis of nanoparticles has been demonstrated to have many advantages over the chemical synthesis of nanoparticles, such as being eco-friendly, cost-effective, efficient, reliable, and non-toxic.

Our study entails the cost-effective synthesis of selenium nanoparticles utilizing microorganisms using banana peel extract (BPE) enriched with tryptophan, as a cheap and alternative source of carbon. We also focus on the stability of the synthesized selenium nanoparticles using BPE when compared to commercially synthesized nanoparticles. These NPs were found to hinder the

neovascularization properties of cell lines and even maintaining the least hemolytic activity at working concentrations. Finally, we have presented the anti-cancer activity of these synthesized nanoparticles on cell lines.

## Materials and Methods

### Chemicals

All the chemicals and media components used in this present study were procured from HiMedia Laboratories (Mumbai, India) and Sigma-Aldrich (USA).

### Cell Lines

HeLa cells were procured from NCCS, Pune, and propagated in DMEM high glucose (Gibco), supplemented with 10% fetal bovine serum and antibiotic antimycotic solution.

### Isolation and Screening of Isolates for the Production of Selenium Nanoparticles

Fresh water sample was collected from the banks of river Krishna, Andhra Pradesh (India) and transported to the laboratory at room temperature. The sample was diluted with sterile distilled water and plated on to Luria agar and incubated at 37 °C overnight. The bacterial isolates were then screened for the production of Selenium nanoparticles by streaking on to Luria agar plates supplemented with 1mM Sodium selenite. These bacterial isolates were stored in 70% glycerol at -80 °C until further use.

### Extraction of Nanoparticles

The nanoparticles were harvested after the incubation period by centrifuging the culture at 12,500 x g for 10 min.<sup>17</sup> The cell pellet was transferred to a 50 mL centrifuge tube, and the pellet was washed using distilled water. A 120 µL of 100 mg/mL lysozyme was added and incubated at 37 °C for 3 h, for cell lysis. The culture was then French pressed at 15,000 psi and centrifuged at 12,500 x g, for 10 min. The pellet was washed with 1.5 M Tris HCl and 1% Sodium Dodecyl Sulphate and centrifuged at 15,000 X g for 10 min. The pellet was resuspended in distilled water and equal amount of Octanol was added and vortexed vigorously for 5 min. The tube was then placed in the fridge overnight. The upper phase and interphase containing insoluble cell fractions were discarded and the aqueous phase containing nanoparticles was transferred to a fresh tube. These nanoparticles were washed with chloroform, absolute ethanol, 70% ethanol and distilled water and suspended in 50 mM tris HCl and stored at 4 °C.

## Identification of Isolate

The morphological characterization of the freshwater isolate was performed according to the methods described by Bergey's manual of determinative bacteriology. Identification of micro-organisms was performed according to the current physiological and biochemical assays, and amplification of bacterial 16S rRNA genes was performed by applying the universal 27F 5' (AGA GTT TGA TCM TGG CTC AG) 3 and 1492R 5' (TAC GGY TAC CTT GTT ACG ACT T) 3' amplified. The following colony was sequenced by Macrogen Inc (Korea).<sup>18</sup> Phylogenetic and molecular evolutionary analyses were conducted using MEGA version X.

## Phenazine Carboxylic Acid Assay

In brief, the isolates were grown for 72 h at 37 °C overnight in 250 mL of LB medium supplemented with 1 mM Tryptophan. The cells were centrifuged at 5000 rpm for 10 min.<sup>19</sup> The cell-free supernatant was collected and acidified with concentrated HCl to achieve a final pH of 2.0. This acidified supernatant was extracted with an equal volume of benzene. The organic phase was collected and dried by placing it in a hot air oven set at 40 °C. This dried residue was dissolved in 1 mL of 0.1 N NaOH. Acidified LB media alone was extracted using benzene and was used as blank in this experiment. The absorbance was recorded at 367 nm. HPLC (Shimadzu) analysis was also performed using C-18 Novapack column with the mobile phase of acetonitrile: water of 70:30 at 254 nm.

## Utilization of Tryptophan Enriched Banana Peel (TEBP) as Alternative Media

Fresh banana peel was collected and washed twice, first with brine solution and then with sterile distilled water. Excess water was drained, and the peels were dried in hot air oven set at 50 °C until no change in the dry weight was observed. The peels were then ground to fine powder and stored at room temperature until further use. Banana Peel extract medium was prepared by first adding the dry powder to 100 mL distilled water and placing it in hot plate set at 80 °C for 30 min under constant stirring.<sup>20</sup> The media were then strained using a muslin cloth and autoclaved at 121 °C for 15 min at 15 lbs pressure. This was used as media for the growth of isolates and for further optimization of parameters for the synthesis of SeNP.

## Downstream Processing

### Optimization of Parameters for Quality Nanoparticle Synthesis

The optimization for quality nanoparticle synthesis was performed by considering 4 parameters ie, pH, selenium concentration, inoculum percentage and incubation time, by using CCD model.

### Experimental Analysis

Here, we designed a single set of experiment with 30 runs having 4 factors ie, pH (A); Selenium concentration (B); Inoculum percentage (C) and incubation time (D) for the optimization of Selenium nanoparticles.

The levels of variables were based on the initial synthesis experiments, wherein Change of One Variable at a Time (COVT) approach was used in both sets. The  $\lambda_{\max}$  was measured in the range of 200–700 nm for SeNP and was used as a response variable ( $Y = RSeNP$ ). The responses from RSM-CCD were subjected to analysis of variance (ANOVA) and second-order multiple regression analysis. This explains the overall behaviour of the system as well as the justification of the significance and adequacy of the developed regression model using the least square regression methodology. Each experimental run of the CCD matrix was analyzed, and the response was correlated with the three input variables by following the quadratic polynomial equation.

$$Y = \beta_0 + \sum_{i=1}^n \beta_i X_i + \sum_{i=1}^n \beta_{ii} X_i^2 + \sum_{i=1}^n \sum_{j=1}^n \beta_{ij} X_i X_j$$

where the parameter is the model constant, and  $\beta_i$  is the linear coefficient;  $\beta_{ii}$ , the quadratic coefficient and  $\beta_{ij}$ , the cross-product (interaction) coefficient.  $X_i$  ( $i = A, B, C$ ) are the independent variables;  $Y$  is the predicted response ( $\lambda_{\max}$  200–700 nm);  $n$  is the number of variables. The 3D graphs, contour plots and the prediction values were used to obtain the optimum conditions required to synthesize better quality SeNP.

### Data Analysis

The design of statistical experiments, analysis of the results, and prediction of the optimum responses ( $\lambda_{\max}$ ) were done by applying the statistical software Design-Expert Version 11.0.0 (State-Ease Inc., Minneapolis, MN, USA).

### Verification of the Model

The process parameters of the biosynthesis of SeNP were numerically optimized by the desirability function of

RSM. The responses were determined under the optimized conditions recommended by the model. Validation of the designed model was done by comparing the model predicted response with the experimental response.

## Characterization of Nanoparticles

### UV-Vis Spectroscopy

The biologically synthesized nanoparticles were studied for surface plasmon resonance using UV-Vis spectroscopy (Epoch, India) at a resolution of 1 nm, at a range of 200–700 nm. Cell mass and cell-free supernatant without adding sodium selenite were used as a control throughout the experiment.

### Fourier Transform-Infrared (FT-IR) Spectroscopy Analysis

FT-IR analysis (SHIMADZU) at a resolution of  $4\text{ cm}^{-1}$ , with a range of  $400\text{--}4000\text{ cm}^{-1}$  in KBr pellets was carried out for the run samples to reveal all the functional groups attached to the surface of biologically synthesized nanoparticles.

### XRD Analysis

The biosynthesized nanoparticles extracted using solvent-based extraction system were dried, and the sample was used for XRD analysis to confirm the crystalline nature of nanoparticles synthesized using Philips X-pert pro, India operated at 40 kV and 30 mA current with 2.2 KW Cu anode radiation ( $k = 1.540\text{ \AA}$ ).

### Scanning Electron Microscopy

The shape and size of the synthesized nanoparticles were analyzed using scanning electron microscopy (Carl Zeiss, AG, India). Samples were loaded on double stick carbon tape, air dried, and documented using different magnifications. The sizes were quantified using the software provided, and EDX analysis of elemental SeNP was carried out with the same instrument at 0–12 keV.

### Zeta Potential Analysis

The effective surface charges on the SeNP at different variables were measured using a zeta analyzer (Horiba scientific, nanoparticles, nanoparticle analyzer SZ-100).

## Cell Viability Assay

The cell viability analysis was performed with the biogenic SeNP isolated using BPE.<sup>21</sup> The HeLa cells were seeded in a 96 well plate at the density of 10,000 cells per well in 200  $\mu\text{L}$  DMEM medium supplemented with 10%

FBS and incubated for 24 h. The wells were replaced with fresh medium, and different concentrations of SeNP were added to each well. Triplicates were maintained for each set of concentration. The cells were incubated for 24 h. The cells were replaced with fresh DMEM medium containing MTT at a final concentration of 0.5 mg/mL. The plate was incubated for 4 h in the dark. The medium was removed, and 100  $\mu\text{L}$  of DMSO was added to each well. The plate was kept in dark for 5 min and the absorbance was measured at wavelength of 570 nm using a microplate reader to calculate cell viability.

$$\text{cell viability (\%)} = \frac{(\text{OD}_{\text{samples}} - \text{OD}_{\text{DMSO}})}{(\text{OD}_{\text{control}} - \text{OD}_{\text{DMSO}})} \times 100$$

## Clonogenic Growth Inhibition Assay

Clonogenic inhibition assay was performed to test the effect of SeNP on HeLa cells.<sup>22</sup> Approximately 1000 cells were seeded onto 6 well plates and treated with different concentrations of SeNP for 24 h. The media was replaced with fresh media after treatment, and the cells were allowed to grow for 7–10 days until each cell was allowed to form a visible colony. The colonies were fixed using 10% neutral buffered formalin for 1 h and then stained with 0.01% crystal violet in distilled water for 1 h. The cells were washed thrice and allowed to dry. The number of colonies formed in each well was counted and the percentage clonogenic growth inhibition was calculated.

## In vitro Cell Migration Assay

To determine the invasiveness of HeLa cells, they were first seeded onto 6 well plates.<sup>23</sup> The cells were seeded until they reached full confluency. The scratch was induced gently using a sterile 10  $\mu\text{L}$  tip onto the surface of 6 well plates. The wells were washed thrice with Dulbecco's Phosphate Buffered Saline. Then, the cells were treated with different concentrations of SeNP. The cells were imaged at 0 h and 24 h timepoint. The scratch width was calculated with ImageJ software, and the scratch width percentage was calculated to determine the cell invasiveness at different concentrations of SeNP.

## Chorio Allantoic Membrane (CAM) Assay

Fertilized 8 days old chick embryos were purchased from Venkateshwara Hatcheries Pvt Ltd, Telangana, India. These

eggs were incubated at 37 ° C under 85% humidity.<sup>24</sup> The eggs were sterilized using surgical spirit, and the blood vessels were marked using an egg candler 1 day prior to inoculation. One hole was made using a sterile needle along the side of the egg. A 10<sup>6</sup> cells were inoculated onto the CAM layer through this hole and later sealed using wax. These cells were further inoculated for 3 days in the incubator. The cells were harvested by break opening the egg shell and separating the CAM layer. The CAM layer was placed onto a petridish, and the neovascularization was quantified by counting the number of blood vessel branch points.

## In vitro Hemolysis Assay

All blood samples used for the study were obtained with the written informed consent of the donor (n=6). Blood hemolysis assay was done on erythrocytes in vitro to assess the hemolytic activity of SeNP.<sup>25</sup> In brief, 1 mL of blood was obtained from a healthy human donor in a 15 mL centrifuge tube containing tri-sodium citrate. This blood was centrifuged at 500 x g for 15 min. The serum was discarded and washed thrice with an equal volume of 1X DPBS. The resulting RBC pellet was resuspended in 50 mL of DPBS for 50 fold dilution. This was considered as stock solution. Different concentrations of SeNP were added to the 1 mL of stock solution of RBC in a 1.5 mL microcentrifuge tube. A 1% SDS was used as a positive control and 1X DPBS was used as the negative control. The reaction mixtures were incubated at 37° C for 24 hr. The absorbance was recorded at 540 nm after the incubation time and the percentage of hemolysis activity was assessed using the following formula:

$$\%, \text{ Hemolytic activity} = \frac{\text{Absorbance of sample} - \text{Absorbance of blank}}{\text{Absorbance of control} - \text{Absorbance of blank}} * 100$$

## Results

### Biosynthesis of Nanoparticles

A total of 13 colonies (K1-K13) were isolated from the water sample. All the isolates were tested for the production of selenium nanoparticles. Among all the isolate, K13 showed better  $\lambda_{\text{max}}$  and color production as compared to other isolates. Hence, this isolate was chosen for our present study.

### Phenazine Carboxylic Acid (PCA) Assay

All the bacterial isolates were checked for the synthesis of phenazine released in the medium. The media of all the isolates was acidified and extracted using benzene and then

dissolved in NaOH. Of all the isolates, only one produced the characteristic peak at around 370 nm as previously reported by<sup>26</sup> Maddula et al 2008. Furthermore, HPLC analysis showed the characteristic peak at a retention time of 9.6 min (Figure 1) for that particular isolate, which is indicative of the presence of phenazine in the medium.

## Identification of Microorganism

The isolate K13 was identified by routine biochemical and morphological examinations followed by 16srRNA sequencing (Macrogen Inc, Korea). The 16srRNA sequence was aligned against the recognized sequences in GeneBank, and it was found to have a homology of 99% with *Pseudomonas stutzeri*. The phylogenetic tree was constructed using MEGA-X software tool using the neighbour-joining method (Figure 2). The sequence was submitted to NCBI (<http://www.ncbi.nlm.nih.gov>) and recorded under the name and accession number MH191156.

## Optimization of BPE Media for Synthesizing Nanoparticles

While optimizing the biological synthesis of nanoparticles, we employed an alternative source of growth medium (carbon and nitrogen-rich source). In this context, we used banana peel extract (BPE) as a cheap nutritional source for the growth of isolated organisms. The isolated strain *Pseudomonas stutzeri* was grown in 8% BPE at pH-6.5 supplemented with 0.25 mM tryptophan. The Np production began after 24 h incubation, as evident from the color production. Nanoparticles of  $\lambda_{\text{max}}$  at 280 nm showed good quality when synthesized using tryptophan enriched BPE. Nanoparticles synthesized using BPE gave a yield of 84%. These nanoparticles were further characterized using different techniques to assess their stability.

## Downstream Processing, Statistical Analysis and Validation

The experiments were conducted in a single set for the statistical analysis and validation of Selenium nanoparticles production using TBPE. The optimum conditions were recorded for analysis. Here, 4 factors were used to run the optimization process. These included pH (4–11.5); Selenium concentration (1–3 mM); Inoculum percentage (15–30%) and Incubation time (24–96 h) (Table 1).

The  $\lambda_{\text{max}}$  of SeNP were confirmed in the treatment runs under the optimum conditions, which were at pH-6.5, selenium concentration of 2 mM, inoculum percentage of 22.5%, and incubation time of 48 h.

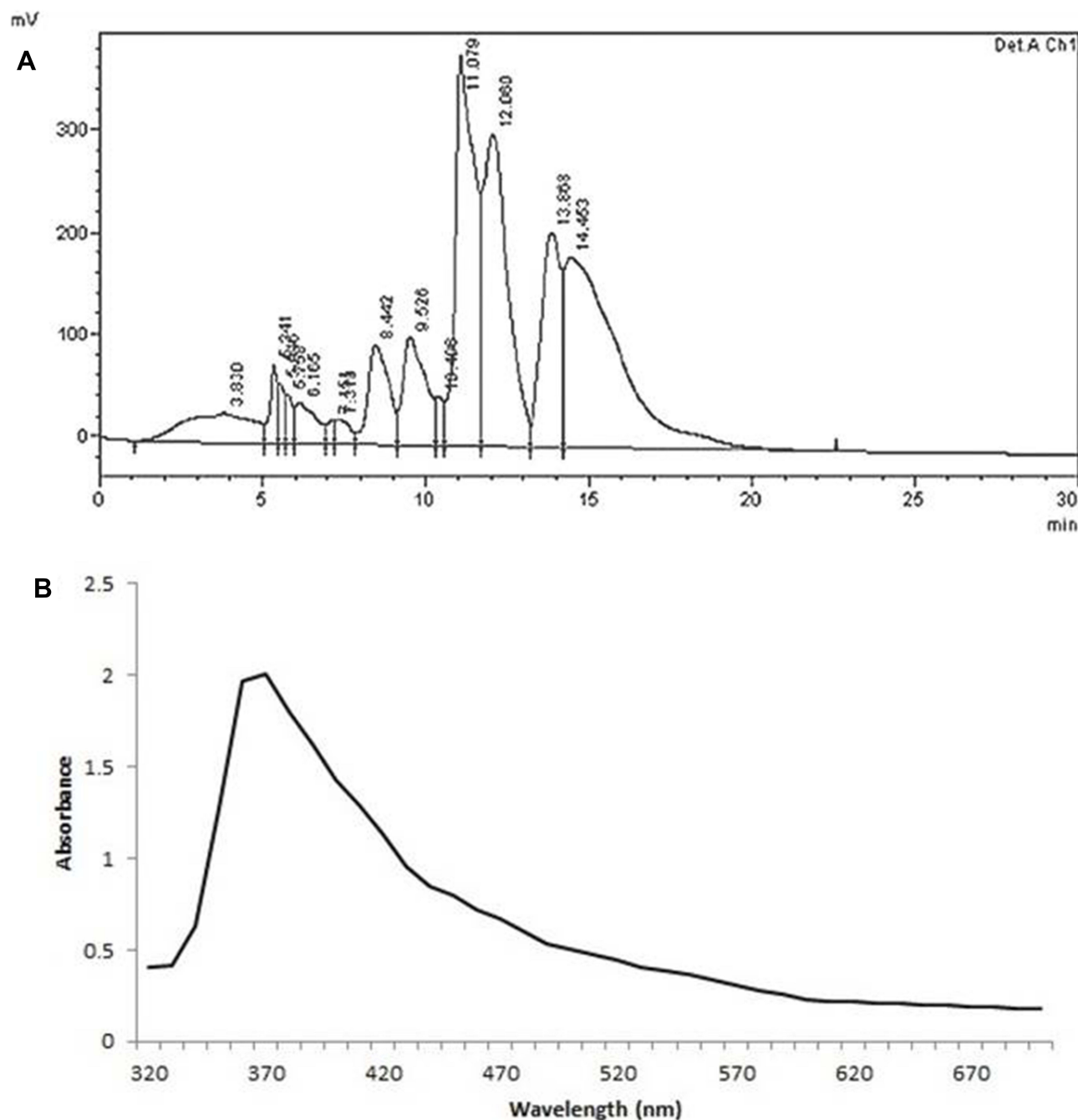


**Figure 1** Phenazine-1 carboxylic acid production by bacteria. Bacterial cultures were grown in presence of Tryptophan. The cell free supernatant was acidified and extracted using benzene. The samples were dried and dissolved in NaOH and **(A)** HPLC analysis revealed characteristic retention time at 9.5. Also, **(B)** UV-Vis spectrophotometer analysis showed an absorption maximum recorded at 370 nm.

The response equation can be written as

$$R1 = +349.33 + 10.04A - 4.29B + 5.21C + 12.79D \\ +13.19AB - 3.69AC - 1.06AD + 0.5625BC - 1.06BD \\ +3.31CD - 19.22A^2 - 12.22B^2 - 12.34C^2 + 0.1563D^2$$

The adequacy of the models was justified by analysis of variance (ANOVA), and the estimated optimum

parameters were computed. The model F value of  $R_{SeNP}$  was calculated to be 3.90, implying that the model is significant for the synthesis of SeNP. The model F-value is the ratio of mean square for the individual term to the mean square for the residual. The Probability > F value is the probability of F-statistics value and is used to test the null hypothesis. The parameters having F-statistical

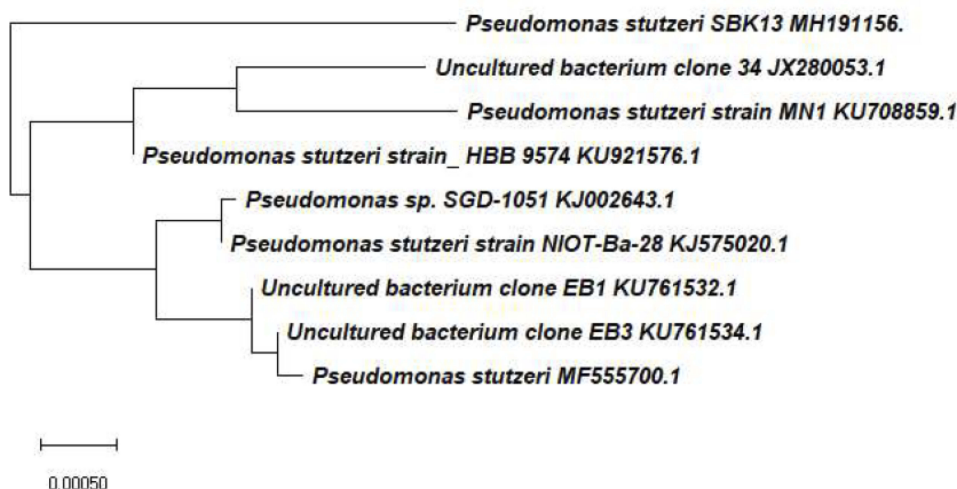


**Figure 2** Phylogenetic analysis. The colony was sequenced for 16S rRNA by Macrogen Inc. The sequence was aligned against sequences from Genbank. The dendrogram of phylogenetic tree was drawn according to 16S rRNA genes by Mega X software ([www.megasoftware.net](http://www.megasoftware.net)).

probability value less than 0.05 are said to be significant, and values greater than 0.1000 indicate the model terms are not significant.

The lack of fit F value of 0.183 and p value of 0.986 (ie, 98.6%) imply that lack of fit is not significant. Relationship between experimental and predicted response values was made based on  $R^2$ , which indicates the relevance of the model for the biosynthesis of nanoparticles. The Predicted  $R^2$  of 0.3499 is not as close to the Adjusted  $R^2$  of 0.5917 as one might normally expect; ie, the difference is more than 0.2. Adequate precision of 7.7 was achieved. This determines the signal-to-noise ratio, where the ratio of 4 or more is considered desirable. The Pred  $R^2$ , ie, the predicted coefficient of determination value, and the Adj  $R^2$ , ie, the adjusted coefficient of determination values, were in reasonable agreement, thereby confirming the significance of the used quadratic model thereby indicating the adequacy of the accuracy of polynomial model and general availability.

Figures 3 and 4 show 3D and contour plots of the synthesized SeNP, respectively. The effects of two parameters for synthesis of nanoparticles were plotted, and the other two parameters were kept constant.<sup>27</sup> These plots clearly show that interactions above and below optimized values resulted in changes in  $\lambda_{\max}$  values. Our data correlates with the optimized predicted variables determined from the CCD model for SeNP synthesis ie, pH 6.5, sodium selenite concentration at 1.75 mM, and incubation time of 48 h.

## Characterization

### FTIR Analysis

FTIR analysis of isolated nanoparticles revealed stretching vibrations in the range of 3400 nm and 1630 nm for all the runs among varied parameters of SeNP. Stretching vibrations at 3400 nm show the presence of O-H bonds of water molecules. The stretching vibrations at 1640 nm show the presence of C=O bonds of amide I of peptide linkage. The bonds indicate the presence of groups on the surface of nanoparticles, which help in the stabilization of nanoparticles. We have found that no variation in the functional groups was observed in SeNP, synthesized using commercial media when compared to different interactions run in RSM-CCD (Figure 5).

### XRD Analysis

The XRD pattern obtained from the SeNP showed a broader pattern without any definite Bragg peaks. Although there were not any strong peaks, small peaks were observed at  $2\theta$  values of 23, 26 and 40 (Figure 6). These data suggest that the SeNP synthesized are not crystalline, rather they are more amorphous in structure.<sup>28</sup> This amorphous nature agrees with the previous studies carried out with *Bacillus sp.*

### Zeta Potential Analysis

Zeta potential analysis was performed to test the stability of synthesized nanoparticles. The zeta potential between +20 and -20 indicates the instability of nanoparticles as lower zeta potential of nanoparticles causes them to aggregate and form clumps. Thus, the greater the charge, the more is the stability of nanoparticles.

**Table 1** Tabular Column Summarizing All the Runs with 4 Parameters Showing pH, Selenium Concentration, Inoculation Percentage, and Incubation Time Along with Absorption Peaks (in nm)

Std	Block	Run	Factor 1	Factor 2	Factor 3	Factor 4	Response 1
			A:pH	B:Se	C:Inoculum percentage	D:Incubation	RI
							nm
17	Block 1	1	6.5	2	22.5	48	330
4	Block 1	2	9	3	15	24	335
5	Block 1	3	4	1	30	24	310
12	Block 1	4	9	3	15	72	335
16	Block 1	5	9	3	30	72	340
2	Block 1	6	9	1	15	24	299
9	Block 1	7	4	1	15	72	310
13	Block 1	8	4	1	30	72	340
8	Block 1	9	9	3	30	24	331
6	Block 1	10	9	1	30	24	310
7	Block 1	11	4	3	30	24	270
3	Block 1	12	4	3	15	24	262
15	Block 1	13	4	3	30	72	313
18	Block 1	14	6.5	2	22.5	48	333
19	Block 1	15	6.5	2	22.5	48	363
10	Block 1	16	9	1	15	72	337
11	Block 1	17	4	3	15	72	280
20	Block 1	18	6.5	2	22.5	48	414
14	Block 1	19	9	1	30	72	333
1	Block 1	20	4	1	15	24	314
26	Block 2	21	6.5	2	37.5	48	305
24	Block 2	22	6.5	4	22.5	48	289
27	Block 2	23	6.5	2	22.5	0	305
21	Block 2	24	1.5	2	22.5	48	260
30	Block 2	25	6.5	2	22.5	48	340
22	Block 2	26	11.5	2	22.5	48	270
28	Block 2	27	6.5	2	22.5	96	380
25	Block 2	28	6.5	2	7.5	48	280
29	Block 2	29	6.5	2	22.5	48	333
23	Block 2	30	6.5	0	22.5	48	297

Zeta potential of values between +20 and -20 is said to be less stable. The stability of nanoparticles from different parameters was selected by testing the surface charge. The nanoparticles showed poor stability when they were synthesized using the commercial media (-14.2 mV), whereas the Nanoparticles synthesized using BPE at a pH of 9, 6.5 and 11.5 showed zeta potential of -39.6, -46.2, and -36.1 mV, respectively (Figure 7). These observations indicate that the nanoparticles synthesized using banana peel extract were found to have better stability when compared with nanoparticles synthesizing using commercial media. Also, the SeNP synthesized at pH of 6.5 was found to have better stability than the SeNP at pH 9 and 11.5.

### SEM and EDX

Selenium nanoparticles produced by the isolated culture grown under different parameters were analyzed for SEM to determine their shape and size. The nanoparticles were spherical in shape when they were synthesized under different pH conditions. A pH of 9.0 showed particle size of about 110–190 nm. At pH 6.5, the particles showed size ranging from 75 to 200 nm. At pH 11.5, particle sizes were found to be 80–200 nm (Figure 8). EDX spectra confirm the presence of Selenium Nanoparticles.

### Comparative Cost Study

We have used both commercial Luria broth and BPE media to synthesize nanoparticles. We have specifically



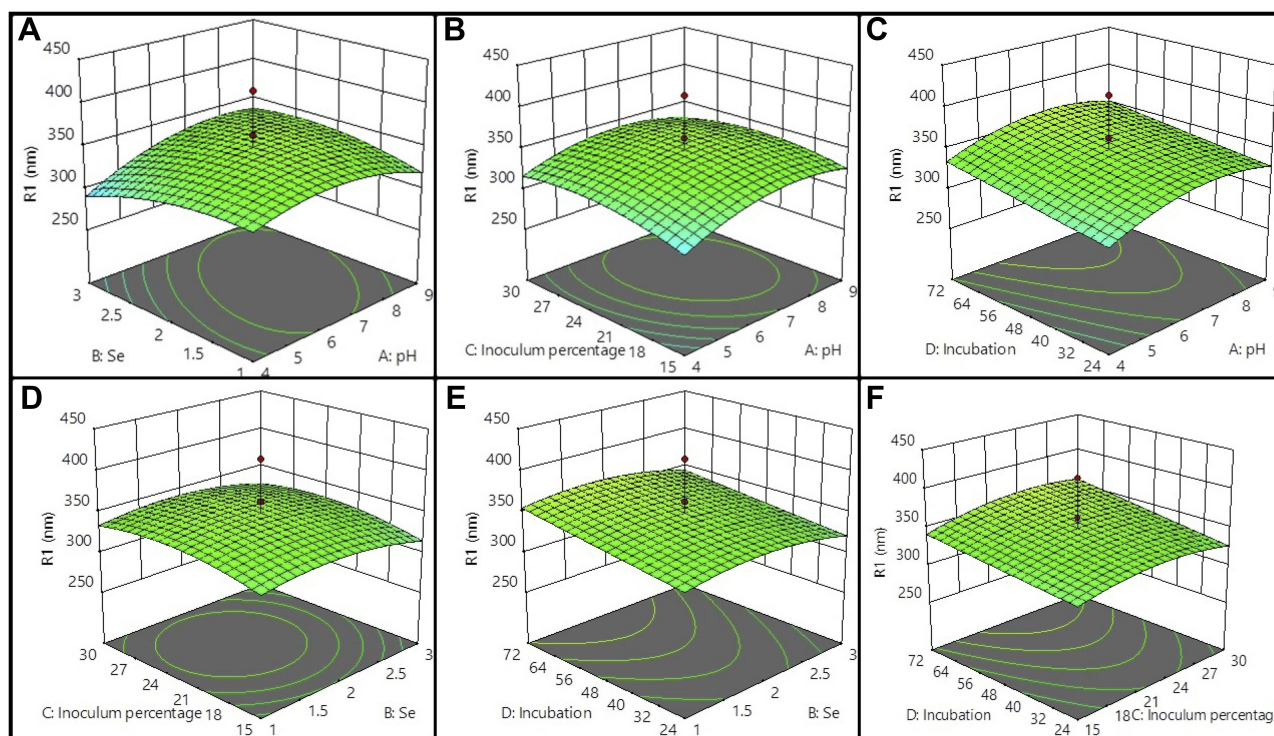


**Figure 3** 3D surface plot analysis. By using Design Expert, 3D surface plots from (A–F) indicate the biosynthesis of SeNP SPR  $\lambda_{max}$  vs all the 4 parameters used in the runs ie, (A) pH, (B) Se concentration, (C) inoculum percentage, and (D) incubation time on different axis. Each plot shows the response values when only 2 parameters are considered, maintaining the other 2 constants.

selected banana peel as a cheap and alternative source of C and N to grow bacteria. By growing the bacteria in BPE and synthesizing the nanoparticles, we not only cut down the cost of production of the nanoparticles, but also found that the nanoparticles were more stable, as evident from the zeta potential values.

#### SeNP-Caused Reduction of the Cell Viability Analyzed by MTT Assay

We have used HeLa cell lines in our present study. We have selected different concentrations (ranging from 200  $\mu\text{g}/\text{mL}$  to 0.5  $\mu\text{g}/\text{mL}$ ) of SeNP for treating cells. HeLa were subjected to different concentrations of selenium nanoparticles ie, 0.5  $\mu\text{g}/\text{mL}$  to 200  $\mu\text{g}/\text{mL}$  for 24 h. In this study, we have found that our biologically synthesized SeNP were found to show cytotoxic effects at a little higher concentration. The cell viability decreased when the concentrations of 5  $\mu\text{g}/\text{mL}$  or above were treated to HeLa cells (Figure 9). However, lower concentrations did not show significant cell cytotoxicity effects.

#### Inhibition of HeLa Cancer Cells by SeNP

To test the antiproliferative effect of SeNP in cancer cells, different concentrations of SeNP were tested in HeLa

cells, and the propensity of individual cells to form a colony was observed and estimated. Anti-proliferative effect of SeNP on HeLa cells was found to be dose-dependent (Figure 10A). The proliferative activity of HeLa cells gradually reduced from 61.4% at 25  $\mu\text{g}/\text{mL}$  to 32.4% at 100  $\mu\text{g}/\text{mL}$  (Figure 10B).

#### Prevention of Cell Migration in vitro by SeNP

The untreated well showed the highest cell migration. These results correlate with the metastasis ability of cell lines. The cells when treated with different concentrations of SeNP showed decreased cell migration. The cell migration decreased by 30% when treated with initial concentration of 5  $\mu\text{g}/\text{mL}$  SeNP. We found that the scratch width was the highest when treated with the highest concentration of SeNP ie, 50 and 100  $\mu\text{g}/\text{mL}$  SeNP (Figure 11). These results indicate the efficacy of our SeNP synthesized using TBPE to prevent the metastasis propensity of HeLa cell lines in vitro.

#### Anti-Angiogenic Activity of SeNP

To test the effect of SeNP on tumour cells, we performed CAM assay in chick embryonated eggs to map

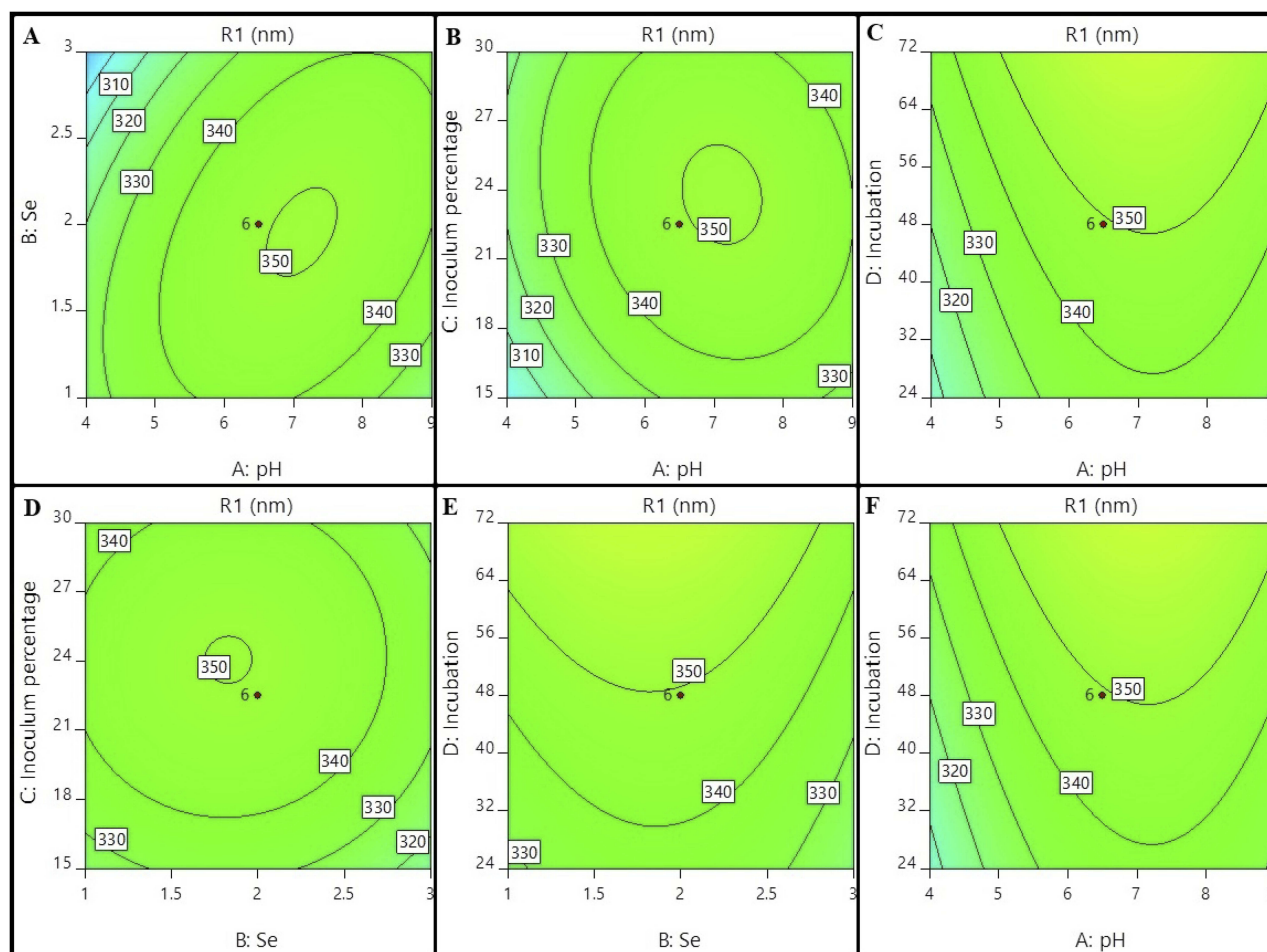


**Figure 4** Contour plot analysis. By using Design Expert, 3D surface plots from (A–F) indicate the biosynthesis of SeNP SPR  $\lambda_{\max}$  vs all the 4 parameters used in the runs ie, (A) pH, (B) Se concentration, (C) inoculum percentage, and (D) incubation time on a different axis. Each plot shows the contour when only 2 parameters are considered, maintaining other 2 constant.

neovascularization. We inoculated CAM of 11-day-old eggs with HeLa cells in the presence SeNP. We found that the number of blood vessels formed increased by 43% in eggs with HeLa cells alone, whereas, the addition of SeNP led to a decrease in angiogenesis by more than 30% (Figure 12). This suggests the potential use of SeNP in preventing neovascularization in tumours.

### Minimum Hemolytic Activity Demonstrated by SeNP

We tested the hemolytic activity of our SeNP synthesized using BPE and SeNP synthesized chemically. Our assay showed 11.5% hemolytic activity at SeNP concentration of 1 mg/mL, decreasing to as low as 4% hemolytic activity of RBC at SeNP concentration of 50  $\mu\text{g/mL}$  (Figure 13). However, the hemolytic activity did not show a significant

change at concentrations lower than 50  $\mu\text{g/mL}$  (data not shown). Chemically synthesized SeNP showed greater haemolytic activity at lower concentrations in comparison to biogenic SeNP. A 0.1% SDS, which was used as a positive control, showed high hemolytic activity as evident from the absorbance and color production. These data suggest that SeNP synthesized is not toxic, even at high concentrations.

### Discussion

A bacterial strain identified as *Pseudomonas stutzeri* was isolated from freshwater samples from banks of Krishna river, India, capable of reducing selenium oxyanions to selenium nanoparticles. Selenium reduction to nanoparticles was observed visually as the color of the media changed to bright red and also by recording  $\lambda_{\max}$  in UV Spectrophotometer.<sup>22</sup> This isolate was shown to produce redox active metabolite, phenazine-1 carboxylic acid that

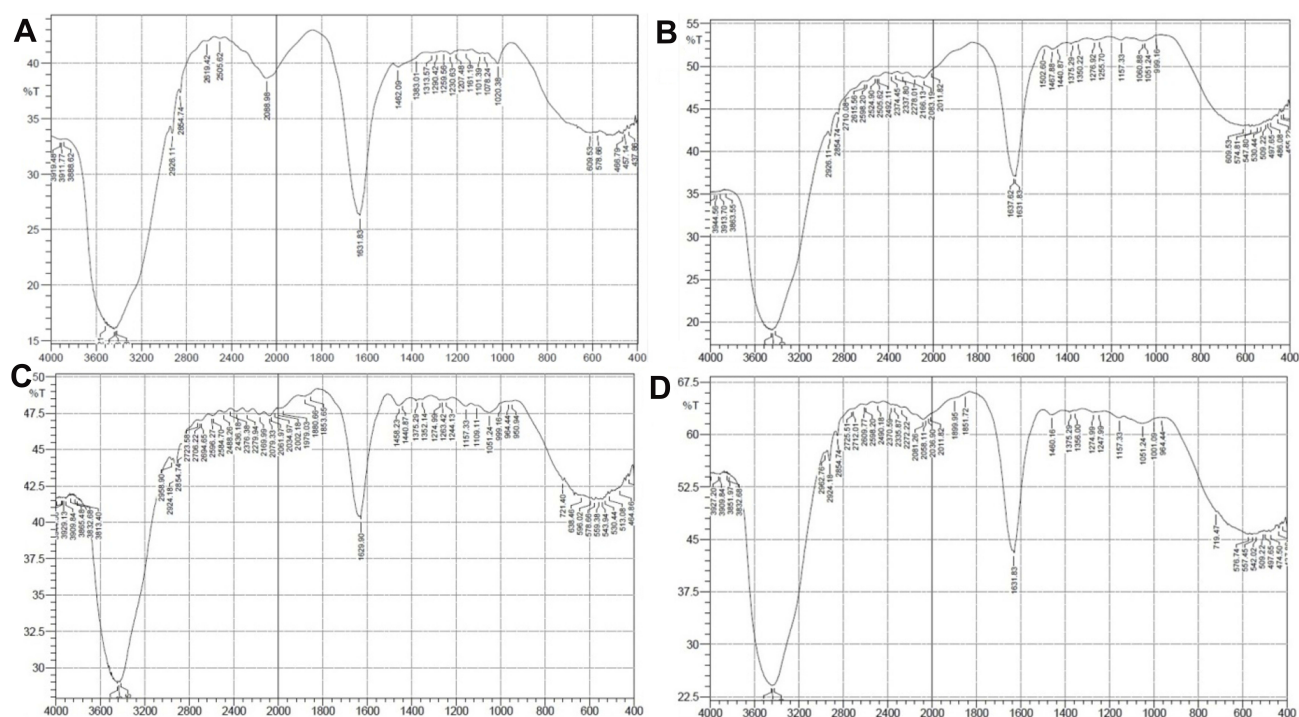


**Figure 5** Fourier transform-infra red analysis of SeNPs. SeNP were extracted from commercial broth and BPE and analyzed for stretching vibrations. The spectrum showed the same stretching vibrations at wavelength of runs with different standardizing conditions using BPE. (A) Nanoparticles synthesized using LB, (B) Np synthesized using BPE at pH 6.5, and (C) pH 9 and (D) pH 11.5.

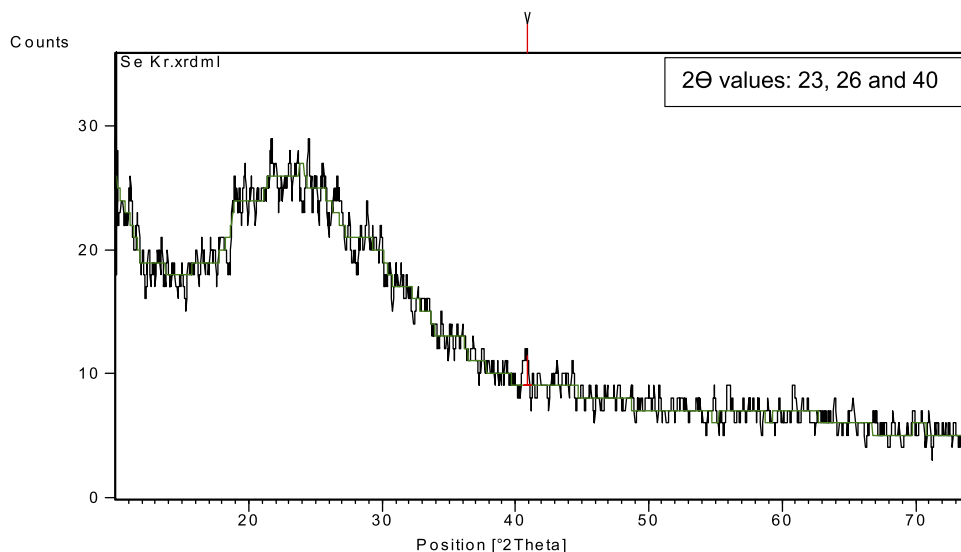


**Figure 6** X-ray diffraction analysis of SeNp synthesized by *Pseudomonas stutzeri*. SeNp synthesized using *Pseudomonas stutzeri* were analyzed by x-ray diffraction. The figure shows undefined broader peaks at  $2\theta$  values of 23, 26 and 40 indicating the amorphous nature of nanoparticles.

helps in reducing the selenium oxyanions to its elemental state. The isolate was grown in the presence of banana peel extract media (BPE 8% and 0.25  $\mu\text{M}$  Tryptophan) as an alternative inexpensive medium to synthesize Selenium nanoparticles. We have employed RSM central composite design (CCD) to analyze downstream processing variables

for the production of Selenium nanoparticles and their effect and interaction. Thus, we required fewer runs and shorter time frames to conduct the study, which is usually sufficient for process optimization. We have also used contour and surface plot for visualization and interaction between variables. The coefficient of determination ( $R^2$ )

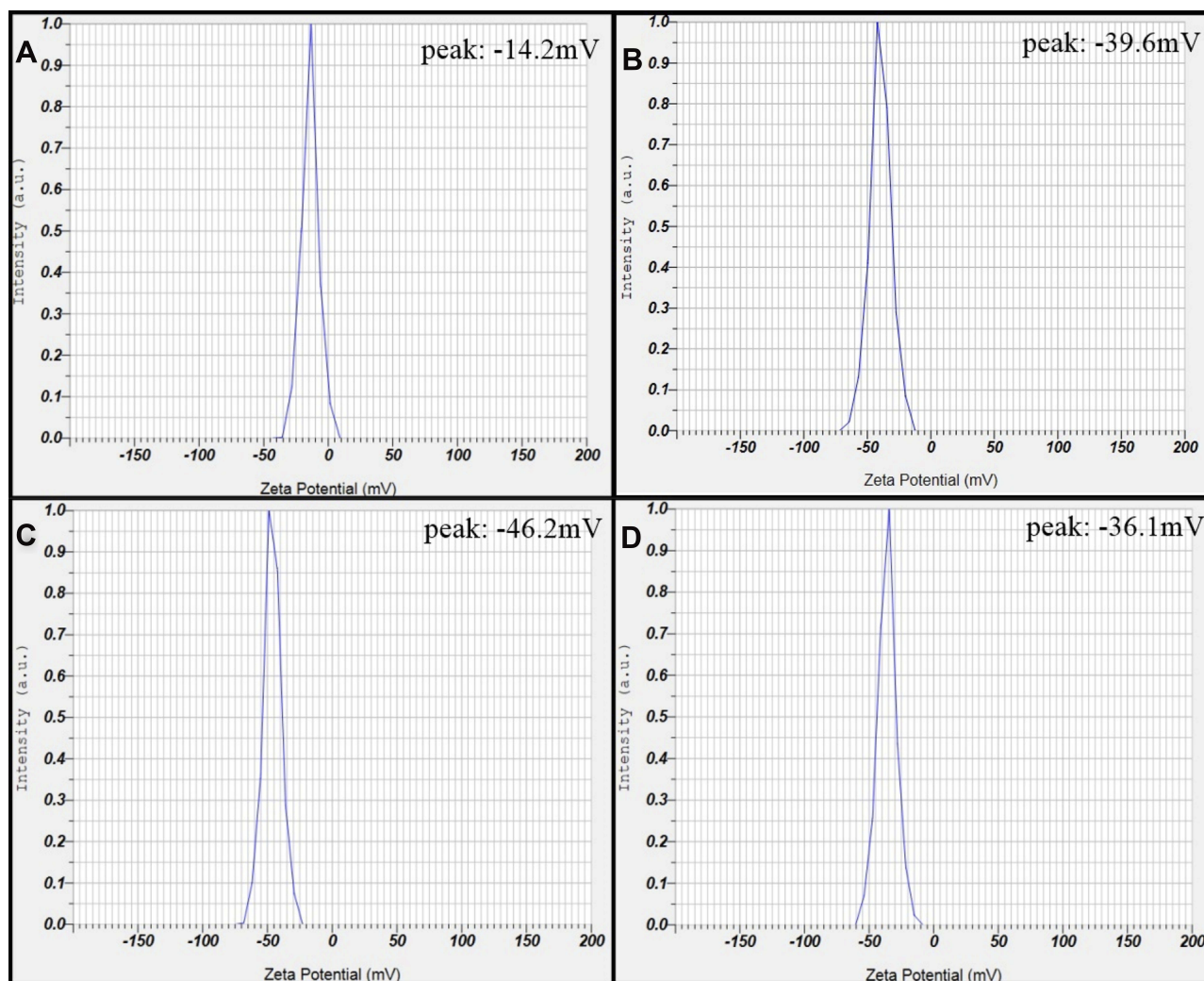


**Figure 7** Measurement of zeta potential of SeNp synthesized by *Pseudomonas stutzeri*. *Pseudomonas stutzeri* (MH) was grown in LB broth or BPE broth, and the culture was used to synthesize SeNp at varying pH values. Figure represents zeta potential values – (A) LB broth (pH 7.2) and the remaining using BPE broth at (B) pH 11.5, (C) pH 6.5 and (D) pH 9, indicating the stability of Nanoparticles at pH 6.5 (–46 mV).

for the model was found to be 0.7959 for the Nanoparticles. The regression model p value was high (ie,  $p < 0.0001$ ), which showed high significance. The isolated nanoparticles were further characterized using XRD and SEM analysis.

By using RSM central-composite design (CCD), we have established optimum parameters required to successfully synthesize the nanoparticles. The optimal condition to synthesize the biogenic selenium nanoparticles was found to be at pH 6.5, selenium at 2%, incubation time of 48 h, and inoculum at 22.5%. FT-IR spectrum revealed the presence of several functional groups that are responsible for reduction and stability of the synthesized nanoparticles. However, similar peaks were observed in FT-IR spectrum of different runs indicating that the nanoparticles had similar functional groups even when the parameters

were changed. The XRD analysis showed no definite peaks, thereby indicating the amorphous nature of selenium nanoparticles. The zeta potential analysis indicated that the nanoparticles synthesized by using BPE were found to be more stable than the nanoparticles synthesized using commercial media (Luria Broth). The nanoparticles were also analyzed using SEM and found to be spherical in shape with size of about 75–200 nm. Thus, our experiments resulted in the production of better stability and uniform nanoparticle size using BPE when compared with those synthesized using commercial media.

Selenium is a trace element known to have antioxidant and anti-tumour activity, although with contradictory conclusions.<sup>29</sup> This is due to the fact that some studies have shown selenium to be pro-oxidant, having

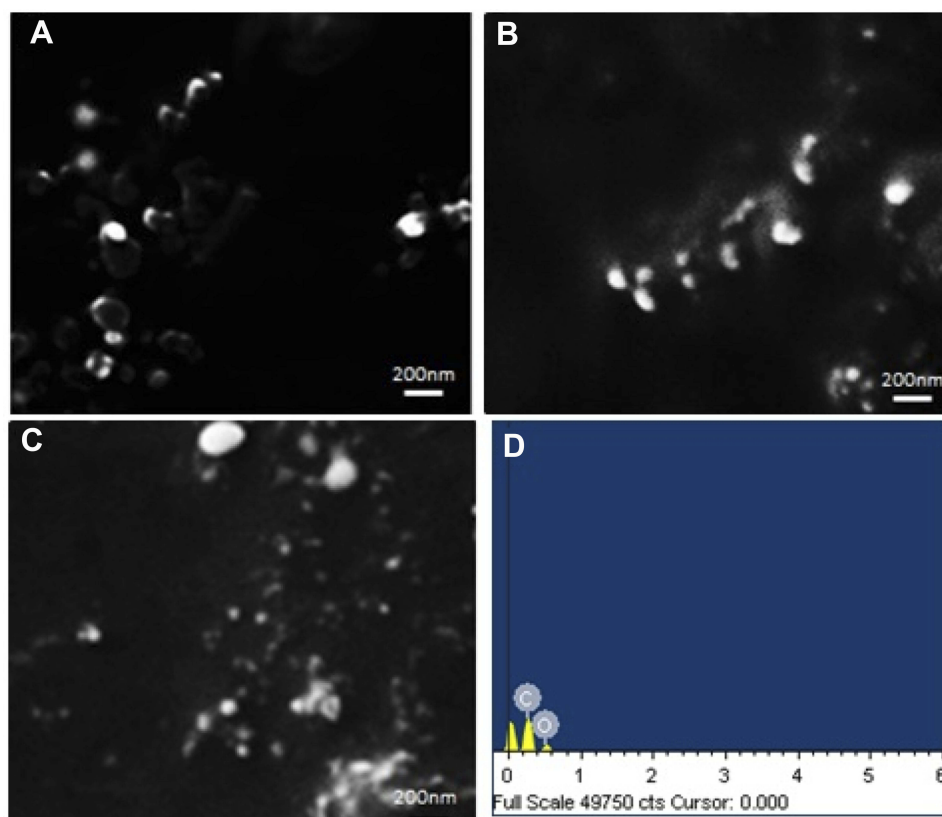


**Figure 8** SEM images of SeNP. The SeNPs synthesized using BPE were extracted using octanol-based extraction at (A) pH 11.5, (B) pH 6.5, (C) pH 9 Showing the average size of 70–200 nm and (D) represents the EDX data that confirms the presence of Selenium.

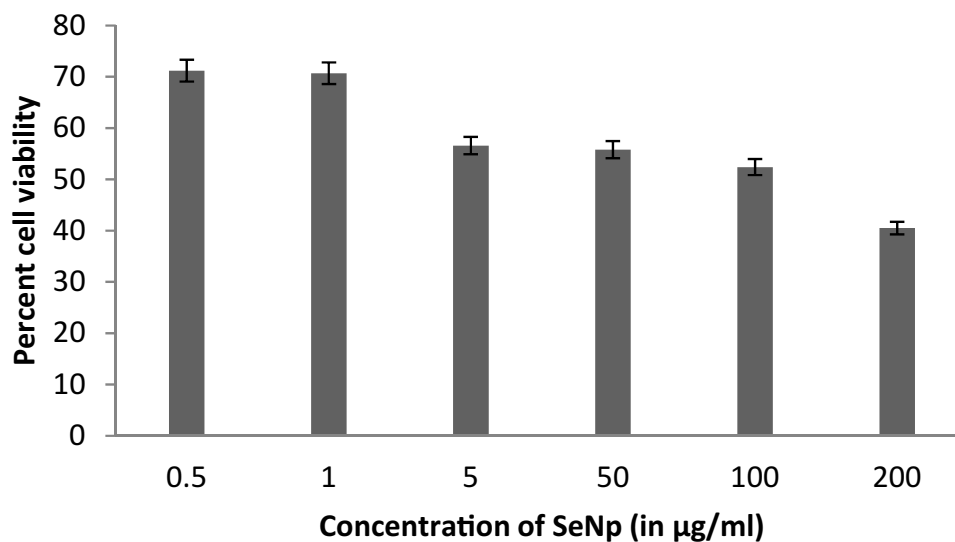


**Figure 9** Cell viability assay of HeLa cells. The cells were treated for 24 h with different concentrations of SeNP in 96-well plate and cell viability was analyzed by its capacity to reduce the formazan dye by checking the absorption maxima at 570 nm. Graph was plotted with concentrations of SeNP (in µg/mL) on x-axis and percent cell viability on y-axis.

a cytotoxic effect on cancer cells by inducing ROS, whereas<sup>30</sup> it is also shown to have an antioxidant role, helping in ROS scavenging.<sup>31,32</sup> Due to its ability to prevent transcription factors like SP1, NF-κB, etc., from

binding to promoter of genes involved in cancer proliferation and metastasis, SeNP can have potential anti-tumour properties.<sup>33</sup> Selenium is known to induce apoptosis in oral carcinomas in caspase-dependent

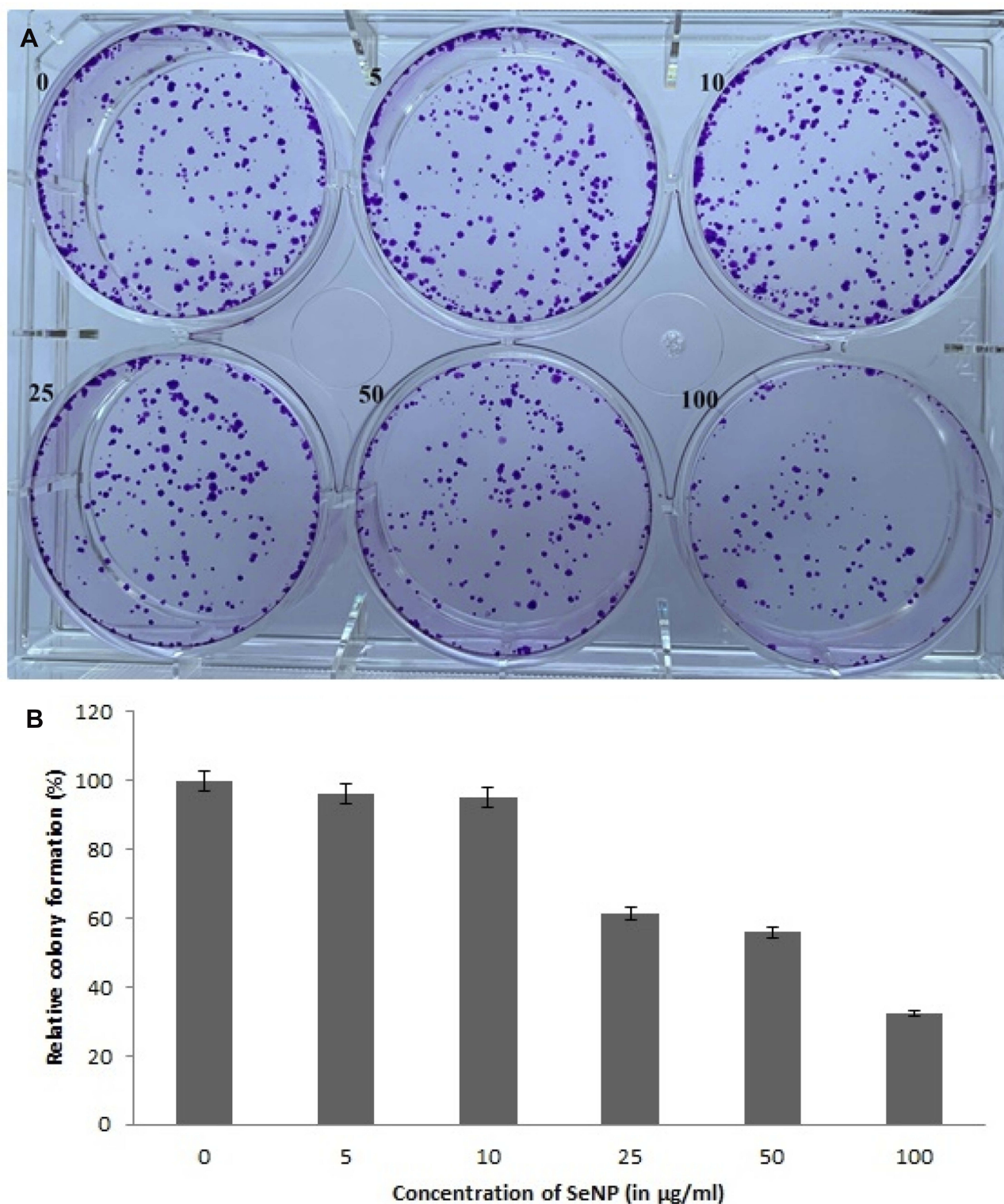


**Figure 10** Clonogenic inhibition of SeNP on HeLa cells. A 1000 cells were treated at different concentrations of SeNP (in µg/mL) in a 6 well plate for 24 h. The media was replaced with fresh media and allowed to grow until each cell became a colony. The cells were stained with crystal violet (**A**) and % clonogenic inhibition of cells with increasing concentration of SeNP was calculated (**B**).

manner through mitochondrial death-receptor and ER stress pathways.<sup>34,35</sup> The toxicity of Se has been shown to be lower in organic and nanoparticle form when

compared with its inorganic counterparts. The effect of Se in all the forms is influenced by several factors including the other components of the compound in

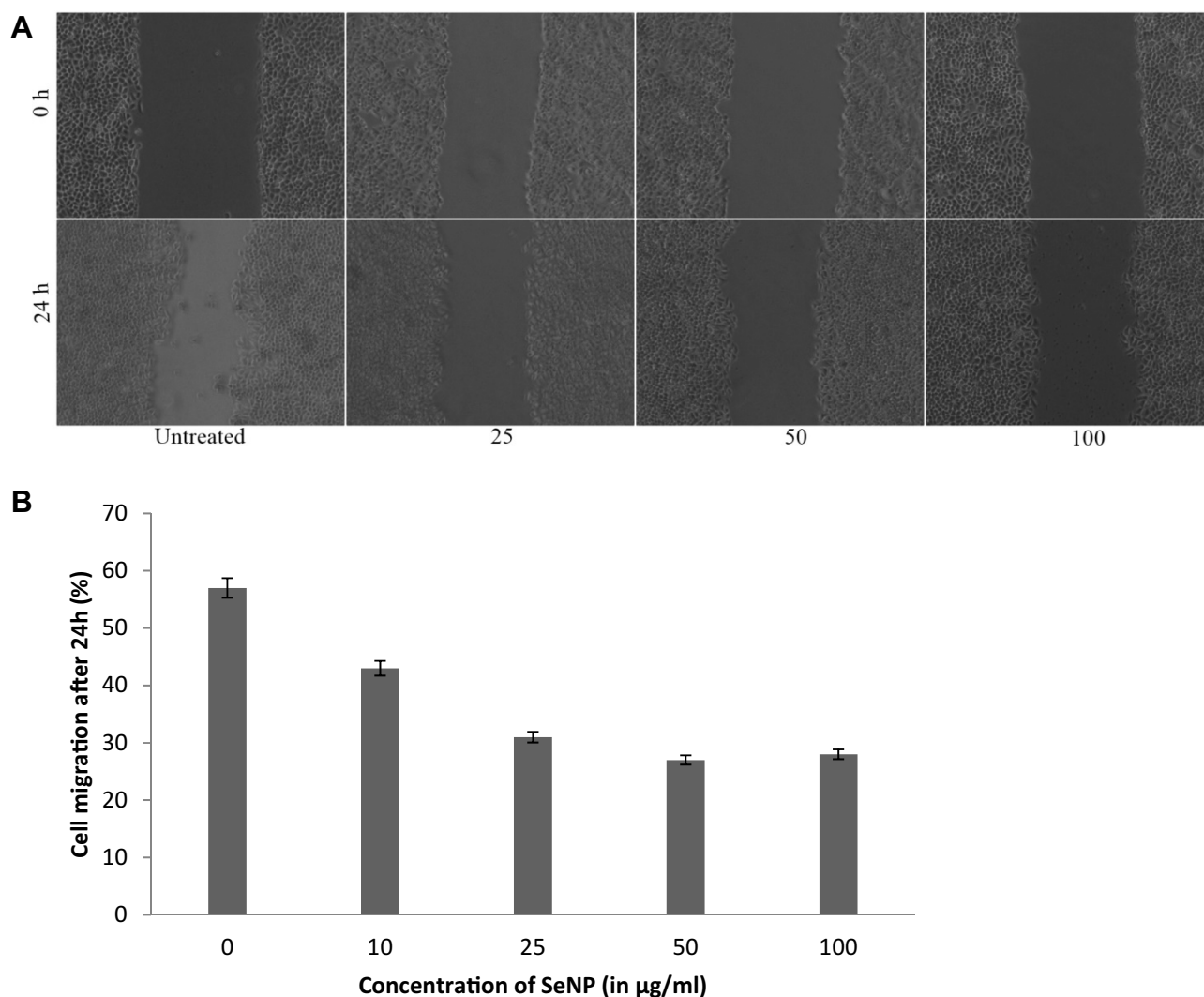


**Figure 11** Measurement of cell migration by in vitro cell migration assay. HeLa cells were grown in 6 well plates to 90% confluency. A scratch was made in the center of the well using a sterile 10 µL tip and the scratch width was measured at 0 h and 24 h time point using ImageJ software. Images were captured with a Thermo Evos inverted microscope at 4X magnification and percentage cell migration was measured. **(A)** Images of scratches made, after 0 h and 24 h treatment at different concentrations of SeNP (in µg/mL). **(B)** Percentage of cell migration after treatment with different concentrations of SeNP was calculated after measuring the scratch width at 24 h with respect to 0h timepoint.

which it is present and also the dose and time for which it is treated. Selenium in its nanoparticle state is less toxic comparatively while preserving its cytotoxicity against tumour cells. Cytotoxicity was observed at a concentration range of 5 µg/mL. To assess the potency of synthesized SeNP at hemolyzing RBC, in vitro hemolytic activity was measured in a dose-dependent manner. Even at higher doses, the NPs were observed to have the least hemolytic effect, thereby indicating low toxicity. To check whether SeNP reduce the proliferative ability of cancer cells, we next performed clonogenic growth inhibition assay. It was observed that SeNP inhibited clono-

genicity of HeLa cells and reduced it by 70%, thereby reducing the propensity for proliferation in presence of SeNP. Also, the time course of the colony formation in treated cells was different from the untreated ones, thereby indicating the reproductive senescence of tumour cells as evident from survival fraction. To check for the effect on invasiveness, we performed in vitro cell migration assay. A dose-dependent reduction in cell migration was observed in SeNP-treated HeLa cells as observed by the prevention of cells from closing the gap caused by the wound/scratch.<sup>36</sup> Hence, these SeNP act by regulating the cell migration through extracellular matrix and cell-

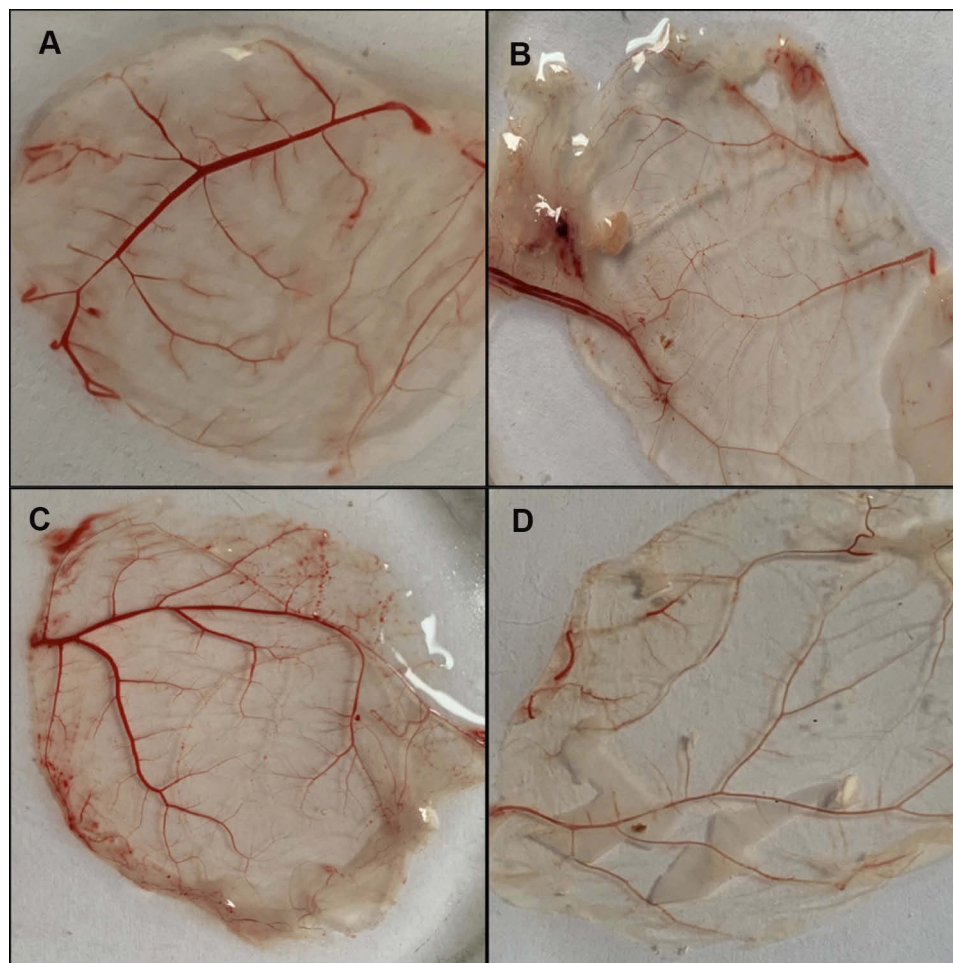


**Figure 12** Analysis of Neovascularization of CAM in the presence of HeLa cells upon treatment with SeNP. Embryonated eggs (11 days old) were inoculated into CAM with HeLa cells in the presence or absence of SeNP and incubated for 3 days at 37 °C. At 3 days, eggs were harvested and changes in angiogenesis in CAM were observed in (A) untreated; (B) HeLa cells (C) when only SeNPs (positive control) were inoculated and (D) when the cells were inoculated in presence of 100µg/mL selenium nanoparticles concentration.

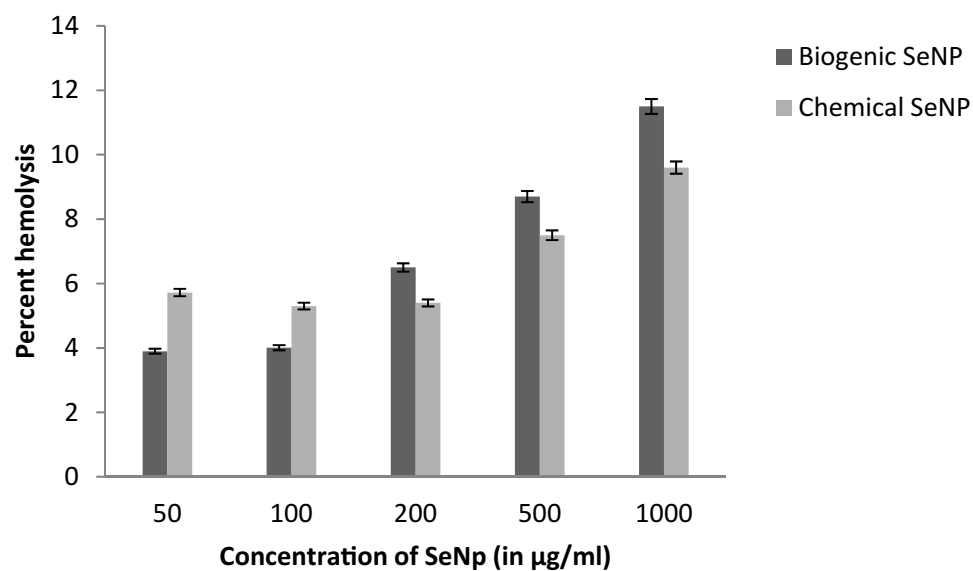


**Figure 13** Analysis of hemolytic activity of selenium Np by in vitro hemolysis assay. Human RBCs were treated with different concentrations of biogenic SeNP and chemically synthesized SeNP, and percentage hemolysis was calculated by measuring absorbance at 540 nm.



cell interactions. Also, neovascularization was reduced by 30% in CAM in the presence of HeLa cells, suggesting its potential use as an anti-angiogenic agent. Overall, the SeNP synthesized have low hemolytic activity combined with significant anti-tumour and anti-angiogenic properties.

## Conclusion

In conclusion, we have optimized the synthesis of SeNP using a freshwater bacterial isolate *Pseudomonas stutzeri* (MH191156) with a lost cost medium formulated at our laboratory. The SeNP thus synthesized showed high stability and uniformity in size. Upon analysis for the biological activity, they were found to have high cytotoxic activity at low concentrations against cancer cells and also exhibited significant anti-tumour and anti-angiogenic properties. Owing to the aforementioned benefits of production cost and extremely favourable anti-tumour properties, these SeNP are potential candidates for further exploration to design effective targeted drug delivery mechanisms.

## Ethical Statement

The study was carried out with the approval of the ethical committee of the Department of Microbiology, University College of Science, Osmania University. Written informed consent was acquired from volunteers for the study. All procedures were conducted in accordance with the declaration of Helsinki.

## Acknowledgments

We would like to thank DST-SERB (YSS/2015/000110), DST PURSE (OU-DST-PURSE-II/44/2018), RUSA 2.0 (MHRD) and UGC-BSR for the financial support of this project.

## Disclosure

The authors report no conflicts of interest in this work.

## References

- MacFarquhar JK, Broussard DL, Melstrom P, et al. Acute selenium toxicity associated with a dietary supplement. *Arch Intern Med*. 2010;170:256–261. doi:10.1001/archinternmed.2009.495
- Menon S, Devi KSS, Santhiya R, Rajeshkumar S, Kumar SV. Selenium nanoparticles: a potent chemotherapeutic agent and an elucidation of its mechanism. *Colloids Surf B*. 2018;170. doi:10.1016/j.colsurfb.2018.06.006
- Jay V, Shafkat R. Antioxidant activity and green synthesis of selenium nanoparticles using *Allium sativum* extract. *Int J Phytomedicine*. 2017;9:634. doi:10.5138/09750185.2185
- Xia Y, Chen Y, Hua L, et al. Functionalized selenium nanoparticles for targeted delivery of doxorubicin to improve non-small-cell lung cancer therapy. *Int J Nanomed*. 2018;13:6929–6939. doi:10.2147/IJN.S174909
- Xia Y, Zhong J, Zhao M, et al. Galactose-modified selenium nanoparticles for targeted delivery of doxorubicin to hepatocellular carcinoma. *Drug Deliv*. 2019;26:1–11. doi:10.1080/10717544.2018.1556359
- Liu T, Zeng L, Jiang W, Fu Y, Zheng W, Chen T. Rational design of cancer-targeted selenium nanoparticles to antagonize multidrug resistance in cancer cells. *Nanomedicine*. 2015;11. doi:10.1016/j.nano.2015.01.009
- Khurana A, Sravani T, Saifi MA, Venkatesh P, Chandraiah G. Therapeutic applications of selenium nanoparticles. *Biomed Pharmacother*. 2019;111:802–812. doi:10.1016/j.biopha.2018.12.146
- Ali EN, EL-Sonbaty SM, Salem FM. Evaluation of selenium nanoparticles as a potential chemopreventive agent against lung carcinoma. *Int J Pharm Biol Chem Sci*. 2013;2:38–46.
- Shakibaie M, Khorramizadeh MR, Faramarzi MA, Sabzevari O, Shahverdi AR. Biosynthesis and recovery of selenium nanoparticles and the effects on matrix metalloproteinase 2 expression. *Biotechnol Appl Biochem*. 2010;56:7–15. doi:10.1042/BA20100042
- Majeed A, Ullah W, Anwar A, et al. Cost-effective biosynthesis of silver nanoparticles using different organs of plants and their antimicrobial applications: a review. *Mater Technol*. 2016:1–8. doi:10.1080/10667857.2015.1108065
- Shankar SS, Rai A, Ahmad A, Sastry M. Rapid synthesis of Au, Ag, and bimetallic Au core-Ag shell nanoparticles using neem (*Azadirachta indica*) leaf broth. *J Colloid Interface Sci*. 2004;275(2):496–502. doi:10.1016/j.jcis.2004.03.003
- Surya S, Kumar GD, Rajakumar R. Green synthesis of silver nanoparticles from flower extract of *Hibiscus rosa-sinensis* and its antibacterial activity. *Int J Innov Res Sci Eng Technol*. 2016. doi:10.15680/IJRSET.2016.0504129
- Gnanajobitha G, Paulkumar K, Vanaja M, et al. Fruit-mediated synthesis of silver nanoparticles using *Vitis vinifera* and evaluation of their antimicrobial efficacy. *J Nanostructure Chem*. 2013;3:1–6. doi:10.1186/2193-8865-3-67
- Bar H, Bhui DK, Sahoo GP, Sarkar P, Pyne S, Misra A. Green synthesis of silver nanoparticles using seed extract of *Jatropha curcas*. *Colloid Surf A-Physicochem Eng*. 2009;348:212–216. doi:10.1016/j.colsurfa.2009.07.021
- Ankanna S, Prasad TNVKV, Elumalai EK, Savithramma N. Production of biogenic silver nanoparticles using *Boswellia ovalifoliolata* stem bark. *Dig J Nanomater Bios*. 2010;5:369–372.
- Parveen K, Banse V, Ledwani L. Green synthesis of nanoparticles: their advantages and disadvantages. *AIP Conf Proc*. 2016;1724:020048. doi:10.1063/1.4945168
- Sonkusre P, Nanduri R, Gupta P, Cameotra SS. Improved extraction of intracellular biogenic selenium nanoparticles and their specificity for cancer chemoprevention. *J Nanomed Nanotechnol*. 2014;5:1000194. doi:10.4172/2157-7439.1000194
- Kumar S, Stecher G, Li M, Knyaz C, Tamura K. MEGA X: molecular evolutionary genetics analysis across computing platforms. *Mol Biol Evol*. 2018;35. doi:10.1093/molbev/msy096
- Dwivedi S, Alkhedhairy AA, Ahamed M, Musarrat J. Biomimetic synthesis of selenium nanospheres by bacterial strain JS-11 and its role as a biosensor for nanotoxicity assessment: a novel se-bioassay. *PLoS One*. 2013;8:e57404. doi:10.1371/journal.pone.0057404
- Ashok B, Joshi B, Kumar AR, Zinjard S. Banana peel extract mediated novel route for synthesis of AgNPs. *Colloid Surf A-Physicochem Eng*. 2010;368:58–63. doi:10.1016/j.colsurfa.2010.07.024
- Jia X, Liu Q, Zou S, Xu X, Zhang L. Construction of selenium nanoparticles/?-glucan composites for enhancement of the antitumor activity. *Carbohydr Polym*. 2015;117:434–442. doi:10.1016/j.carbpol.2014.09.088

22. Kirwale S, Pooladanda V, Thatikonda S, Murugappan S, Khurana A, Godugu C. Selenium nanoparticles induce autophagy mediated cell death in human keratinocytes. *Nanomedicine*. 2019;14(15):1991–2010. doi:10.2217/nnm-2018-0397
23. Justus CR, Leffler N, Ruiz-Echevarria M, Yang LV. In vitro cell migration and invasion assays. *J Vis Exp*. 2014;88:e51046. doi:10.3791/51046
24. Naik M, Brahma P, Dixit M. A cost-effective and efficient chick ex-Ovo CAM assay protocol to assess angiogenesis. *Method Protoc*. 2018;1:19. doi:10.3390/mps1020019
25. Cheng C, Yin C, Chung Y, Shun C, Ken CM, Peter Y. In vitro cytotoxicity, hemolysis assay, and biodegradation behavior of biodegradable poly(3-hydroxybutyrate)-poly(ethylene glycol)-poly(3-hydroxybutyrate) nanoparticles as potential drug carriers. *J Biomed Mater Res*. 2008;87(Part A):290–298. doi:10.1002/jbm.a.31719
26. Maddula VSRK, Pierson EA, Pierson LS. Altering the ratio of phenazines in *Pseudomonas chlororaphis* (aureofaciens) strain 30–84: effects on biofilm formation and pathogen inhibition. *J Bacteriol*. 2008;190:2759–2766. doi:10.1128/JB.01587-07
27. Fesharaki PJ, Nazari P, Shakibaie M, et al. Biosynthesis of selenium nanoparticles using *Klebsiella pneumoniae* and their recovery by a simple sterilization process. *Braz J Microbiol*. 2010;41(2):461–466. doi:10.1590/S1517-83822010000200028
28. Chandramohan S, Sundar K, Muthukumaran A. Monodispersed spherical shaped selenium nanoparticles (SeNPs) synthesized by *Bacillus subtilis* and its toxicity evaluation in zebrafish embryos. *Mater Res Express*. 2018;5(2):025020. doi:10.1088/2053-1591/aaabeb
29. Wallenberg M, Misra S, Wasik AM, et al. Selenium induces a multi-targeted cell death process in addition to ROS formation. *J Cell Mol Med*. 2014;18. doi:10.1111/jcmm.12214
30. Zhou YJ, Zhang SP, Liu CW, Cai YQ. The protection of selenium on ROS mediated-apoptosis by mitochondria dysfunction in cadmium-induced LLC-PK1 cells. *Toxicol in Vitro*. 2009;23:288–294. doi:10.1016/j.tiv.2008.12.009
31. Gasparian AV, Yao YJ, Lü J, et al. Selenium compounds inhibit IκB kinase (IKK) and nuclear factor-κB (NF-κB) in prostate cancer cells. *Mol Cancer Ther*. 2002;1:1079–1087.
32. Chun JY, Hu Y, Pinder E, Wu J, Li F, Gao AC. Selenium inhibition of survivin expression by preventing Sp1 binding to its promoter. *Mol Cancer Ther*. 2007;6:2572–2580. doi:10.1158/1535-7163.MCT-07-0172
33. Manabu E, Hiroshi H, Tetsuharu K, et al. Antitumour activity of selenium compounds and its underlying mechanism in human oral squamous cell carcinoma cells: a preliminary study. *J Oral Maxillofac Surg Med Pathol*. 2016;29. doi:10.1016/j.ajoms.2016.08.006
34. Hosnedlova B, Kepinska M, Skalickova S, et al. Nano-selenium and its nanomedicine applications: a critical review. *Int J Nanomedicine*. 2018;13:2107–2128. doi:10.2147/IJN.S157541
35. Wadhvani S, Shedbalkar U, Singh R, Chopade B. Biogenic selenium nanoparticles: current status and future prospects. *Appl Microbiol Biotechnol*. 2016;100. doi:10.1007/s00253-016-7300-7
36. Liang C-C, Park A, Guan J-L. In vitro scratch assay: a convenient and inexpensive method for analysis of cell migration in vitro. *Nat Protoc*. 2007;2:329–333. doi:10.1038/nprot.2007.30

International Journal of Nanomedicine

Dovepress

## Publish your work in this journal

The International Journal of Nanomedicine is an international, peer-reviewed journal focusing on the application of nanotechnology in diagnostics, therapeutics, and drug delivery systems throughout the biomedical field. This journal is indexed on PubMed Central, MedLine, CAS, SciSearch®, Current Contents®/Clinical Medicine,

Journal Citation Reports/Science Edition, EMBase, Scopus and the Elsevier Bibliographic databases. The manuscript management system is completely online and includes a very quick and fair peer-review system, which is all easy to use. Visit <http://www.dovepress.com/testimonials.php> to read real quotes from published authors.

Submit your manuscript here: <https://www.dovepress.com/international-journal-of-nanomedicine-journal>